

Energy of Ions in Vacuum Arcs between Axial and Radial Magnetic Field Contacts

G. Düning, M. Lindmayer

Technische Universität Braunschweig
Institut für Hochspannungstechnik und Elektrische Energieanlagen
Postfach 3329, 38023 Braunschweig, Germany

Abstract

In vacuum circuit breakers two different contact types are used to overcome the consequences of arc constriction, which sets in when currents of several kiloamperes are exceeded. Radial magnetic fields (RMF) force the constricted arc to rotate and distribute its power more evenly on the contact surface. Axial magnetic field (AMF) contacts prevent the arc from becoming constricted up to higher thresholds. To improve the interruption capability of vacuum circuit breakers of both types it is essential to know about the processes and properties of the vacuum plasma ("vacuum arc") around current zero, such as plasma density and its decay and the energy of the plasma species. In this work the energy distribution of ions in the vacuum arc plasma during the last 3 ms before current zero has been investigated by means of a retarding field analyzer up to arc currents of 7.5 kA RMS. Significant differences could be observed between RMF and AMF contacts. For currents above 5 kA the distribution in both cases resembles a Maxwellian distribution, characteristic for a collision-determined plasma. On lower currents, i.e. when current zero is approached, RMF arrangements show ions with strongly directed motion, while the energy distribution for AMF contacts is much more influenced by collisions.

1. Introduction

In vacuum circuit breakers two different contact types are used to overcome the consequences of arc constriction, which sets in when currents of several kiloamperes are exceeded. On the one hand, contacts generating radial magnetic fields (RMF-contacts) force the arc to rotate and distribute its power more evenly on the contact surface. Disks with spiral slots are one possible design of such RMF contacts [1,2]. On the other hand, AMF-contacts creating an axial magnetic field, prevent

the arc from becoming constricted up to higher thresholds. Independently of the used contact type the vacuum arc is in the state of a diffuse arc mode for currents below a few kA. In this mode the processes on the cathode are characterized by single cathode spots as the source of emitted metal vapor and electrons [3]. The metal vapor, ionized by the electrons accelerated in the electric field near the cathode, builds a positive space charge sheath between the cathode surface and the neutral plasma [4]. Due to the acceleration by the high pressure gradient, the friction between ions and electrons and the electric field the plasma ions expand with high kinetic energy from the cathode region to the anode [5]. The value of this ion current opposite to the voltage polarity of the external circuit lies in a range of 7 - 10% of the total arc current [6].

For mathematical models of the vacuum arc and its extinction it is of interest to know the density and energy distribution of the plasma as it approaches current zero. The ion energy distribution, which is the subject of this paper, can be determined by a retarding field analyzer [7,8,9]. It is based on the separation of the ions from the electrons by metal grids, applied with a negative voltage and the retarding field by the collector, biased by a voltage higher than the plasma potential [10]. According to [11] the average ion energy value depends on the value of the arc current, the peak values of the ion energy shifting towards higher energies with a decreasing arc current [11]. This tendency has also been shown for high current 50 Hz switching arcs between RMF contacts by Rusteberg [7,8]. In this present work the determination of ion energies is extended towards AMF contacts in order to learn about significant differences between these basic arrangements. The data on RMF contacts given here for comparison are mainly taken from [7].

2. Experimental circuit and retarding field analyzer

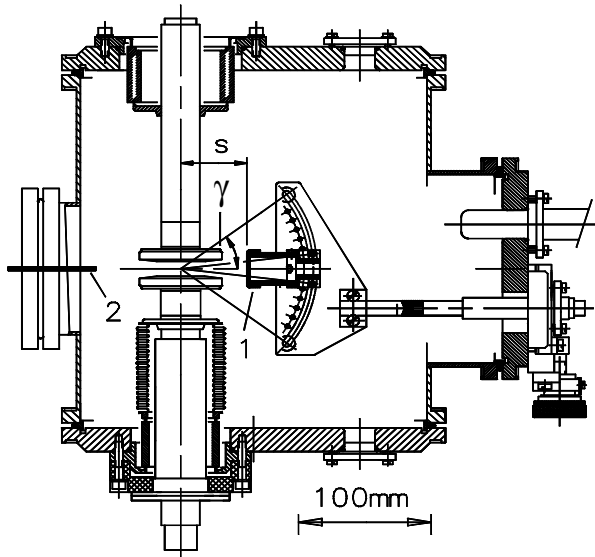


Fig. 1: Model switch with main contacts, retarding field analyzer (1) and Langmuir probe (2)

The experiments were carried out in a special model switch according to fig. 1. The sinusoidal half-wave currents between $1 \text{ kA}_{\text{RMS}}$ and $7.5 \text{ kA}_{\text{RMS}}$ and with a frequency of 50 Hz were generated by an LC circuit, consisting of a bank of 3 kV-capacitors in series with inductances. In the experiments this current is made by an external closure switch. The contacts are opened shortly ($< 2 \text{ ms}$) afterwards, thus giving an arcing time until next current zero between 8 and 10 ms. In all the experiments the upper fixed contact represents the high-current anode while the movable lower contact is the cathode. Initiating the vacuum arc by contact opening one millisecond after the beginning of current flow by a pneumatic actuator (not shown) with an average velocity of 1.7 m/s makes sure that the cathode-contact has reached its end-position 3.5 to 4 ms before current zero. The RFA measurements are carried out only in the last 3 ms before current zero. The main parameters of the different contact-types are shown in table 1.

Table 1 - contact parameters

	RMF contacts	AMF contacts
Contact type	RMF-Type 1 [1]	AMF-Type A [2]
Diameter	62 mm	62 mm
Material	CuCr 72/25	CuCr 75/25
Gap distance	12 mm	12 mm

During all the experiments the cathode was grounded while the stainless steel vessel of the model switch was floating. The measured potentials refer to the cathode potential. By a permanent connection to a turbo molecular pump a total pressure below 10^{-5} Pa is maintained.

The plasma parameters were measured by using the Retarding Field Analyzer (RFA) as shown in fig. 1 with its position in sight to the main contacts and the arc-gap. The "viewing angle" γ can be varied in steps of 5° . $g = 0^\circ$ is the position orthogonal to the contact axis. Positive g means that the analyzer "looks" onto the cathode. The distance s between the contact axis and the surface of the aperture of the RFA is varied in steps of 5 mm between 50 and 110 mm.

The scheme of the RFA is shown in fig. 2. It consists of an metal housing, the aperture in visual line to the contacts and the vacuum plasma between them, two metal grids for electron separation and the collector for the ion detection [7].

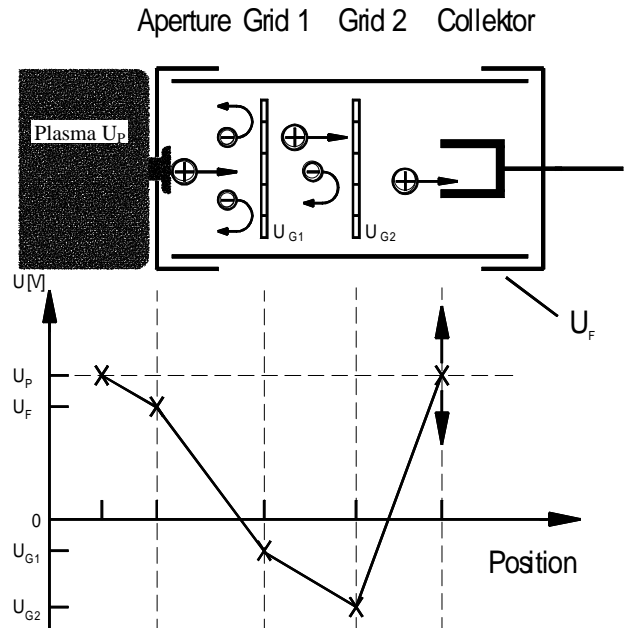


Fig. 2: Retarding field analyzer with potential distribution and plasma

Through the aperture the plasma, mainly consisting of positive ions and electrons, gets into the RFA. The housing and the aperture of the RFA are on floating potential U_f during the experiments. For the determination of the ion potential it is necessary to separate the plasma ions from the electrons.

Therefore the two nickel grids were used. The wires of the grids had a diameter of $2r = 0.02$ mm and a spacing between the wire axes of $d = 0.1$ mm. By applying a negative voltage between 10 and 15 V on the two grids the electrons are repelled by the electric field.

As explained in detail in [7,8], for an efficient separation certain conditions must be fulfilled concerning the dimensions of the grid mesh and the Debye length of the plasma within the analyzer. As the arc plasma density varies with the arc current [7,11], a current-dependent adjustment of the density had to be made for optimal separation by different diameters of the aperture hole. Assuming constant ion speed in the orifice the density of the plasma within the analyzer is inversely dependent on the orifice diameter, as was also shown experimentally in [7,9].

After passing the separation area of the two grids the ions fly against the retarding field of the collector. The collector voltage U_C is varied in steps of 5 V between -10 and +70 V related to the cathode. In accordance to the collector voltage U_C the ion current consists only of those high energy ions with a sufficient speed to surmount the retarding field. The ion potential distribution is determined by measuring the ion current I_C and the collector voltage U_C . A typical I_C - U_C - characteristic of the RFA is shown in fig. 3. It can be divided in three different areas.

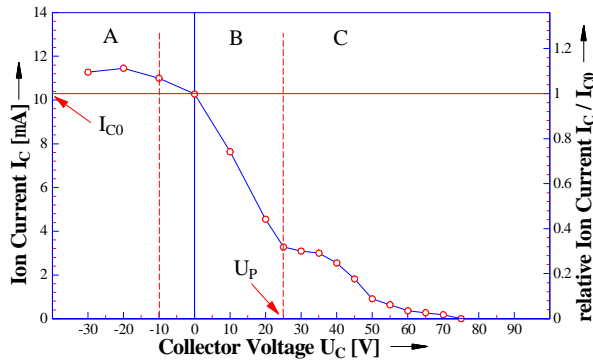


Fig. 3: I_C - U_C - characteristic of RMF-contacts ($I_B = 1.75$ kA_{RMS}, $U_{G1} = -10$ V, $U_{G2} = -15$ V, $g = 0^\circ$, $s = 50$ mm)

Section A:

In the saturation area the collector voltage is much lower than the plasma potential, therefore all ions which reach the analyzer are accelerated towards the collector. For the collector voltage $U_C = 0$ V the ion current I_C is defined as the

ion saturation current I_{C0} . It depends on the ion density n_i , the diameter of the orifice and the transparency of the separation grids.

Section B:

The transition area is characterized by the strong decrease of the ion current I_C with increasing collector voltage U_C . If the collector voltage approaches the plasma potential U_P the acceleration of the ions towards the collector stops. The plasma potential is determined by a separate Langmuir probe measurement.

Section C:

In the retarding area the ions that fly to the collector are repelled by the retarding field between the separation grid 2 and the collector. For this case, the collector voltage U_C must be higher than the plasma potential U_P .

Because of the non-monochromatic character of the ion energies (= ion speeds) the retarding curve in section C reflects the ion energy distribution. [7,8,12]

When the ion energy is related to the plasma potential at the location of the analyzer, the dependence between the collector current and the ion energy distribution is given by

$$I_C = c_1 \cdot \int_{W=e(U_C-U_P)}^{\infty} f(W_i) dW_i \quad (1)$$

$$W_i = U_C \cdot Z \cdot e \quad (2)$$

I_C	ion current
U_C	collector voltage
U_P	plasma potential
W_i	ion Energy
c_1	Integration constant
e	electron charge
Z	mean ion charge state, typically 1.8 [13]

The distribution function $f(W_i)$ of the ion energy can be derived by numerical differentiation:

$$f(W_i) = \frac{1}{c_2} \cdot \frac{dI_C}{dU_C} \quad (3)$$

For all the described measurements and results the separation grids were supplied with constant voltages ($U_{G1} = -10$ V, $U_{G2} = -15$ V), the orifice diameter could be kept constant for the measurements with arcs on AMF-contacts, but it had to be varied for RMF-contacts to adapt for an optimal separation.

3. Measurements and results

3.1 General

Fig. 4 shows the ion current I_C with its typical shapes for different collector voltages U_C . Each trace originates from a different switching experiment. Additionally the arc current I_B and a typical evolution of the floating potential U_F of the RFA housing are shown.

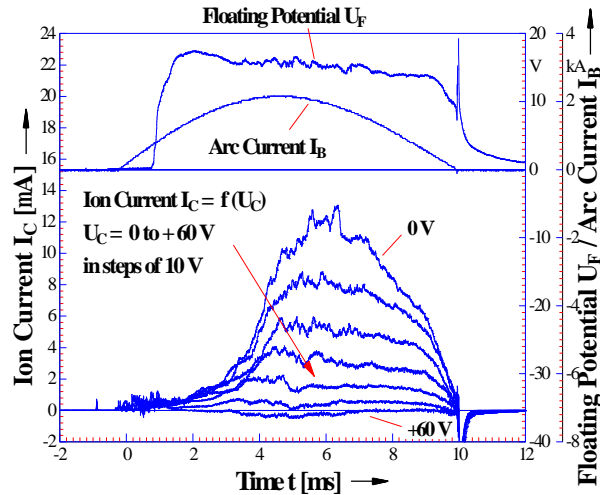


Fig. 4: Typical ion currents I_C with $I_C = f(U_C)$, $U_C = 0$ to $+60$ V, $I_B = 2$ kA_{RMS}, $g = 0^\circ$, $s = 50$ mm, AMF-contacts

The contact opening is characterized by the strong increase of the floating potential U_F one millisecond after the beginning of the arc current flow. The ion currents are typically characterized by their sharp increase 3 ms after contact opening. At this time the surface of the arc cathode (movable contact) passes the visual line of the RFA. In coherence with the decreasing ion density n_i according to the decrease of the arc current, the ion current decreases in the last 3 ms before current zero.

With increasing collector voltage and retarding field, respectively, the ion current decreases. The maximum ion current shown in the diagram for $U_C = 0$ V represents the ion saturation current I_{C0} . For a collector voltage $U_C = +60$ V no further ions can be detected during the last 3 ms before current zero.

From this kind of measurements typical I_C - U_C - characteristics as shown in fig. 5 can be depicted, both in linear milliamper scale and in semi-logarithmic scale related to I_{C0} . The parameter is the time before current zero. The shorter this interval, the smaller is the momentary arc current.

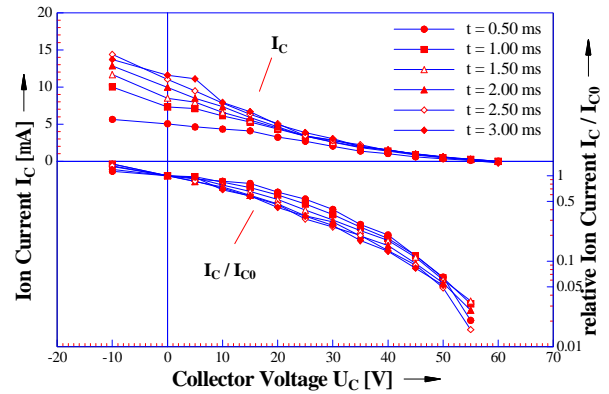


Fig. 5: I_C - U_C - characteristic of AMF-contacts ($I_B = 2$ kA_{RMS}, $U_C = -10$ to $+60$ V, $g = 0^\circ$, $s = 50$ mm, $t = 3.0$ to 0.5 ms before current zero)

Every point shown in the curves is the average of ten points from separate identical experiments. The collector voltage U_C was changed in 5 V steps. Obviously there are ions with considerably higher potentials (=energies) than the plasma potential of approximately 20 V.

In comparison with the typical characteristic for RMF-contacts (fig. 3) the characteristic for AMF-contacts cannot be separated in the three distinct areas. The curves show no marked saddles but fall rather monotonously.

The energy distribution was determined by fitting the measured points in logarithmic representation (figs. 3, 5 etc.) with a third order polynomial function and by analytical differentiation of this function. While for the collector voltages the cathode potential is the basis ($V=0$), the plasma potential on the location of the analyzer, which lies definitely higher, is taken as basis for the energy distribution, i.e. the plasma potential has to be subtracted from the retarding collector voltage. It was determined by the standard method

with an extra Langmuir probe. These experiments on AMF-contacts for currents from 1 to 7.5 kA_{RMS} and times before current zero between 3 and 0.25 ms showed only narrow plasma potential variations around 20 V, whereas experiments with RMF-contacts [7] show a much wider distribution of the plasma potential depending on the arc current.

3.2 Ion energy distribution of arcs between RMF- and AMF-contacts

The differences already mentioned of the typical I_C-U_C -characteristics between RMF- and AMF-contacts are shown in fig. 6a and 6b, both representing the relative ion current I_C / I_{C0} in a semi-logarithmic plot.

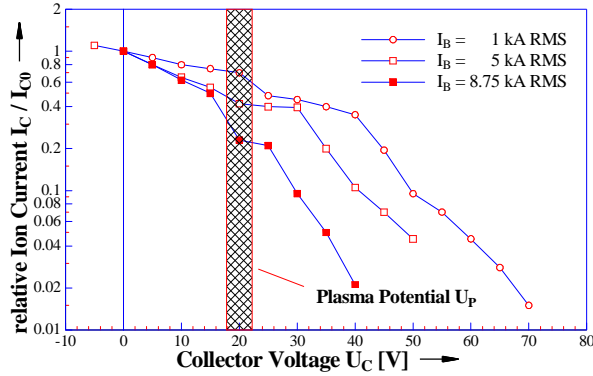


Fig. 6a: I_C-U_C -characteristics for RMF-contacts ($I_B = 1$ to 8.75 kA_{RMS}, $U_C = -5$ to +70 V, $g = 0^\circ$, $s = 50$ mm, $t = 2.5$ ms before current zero)

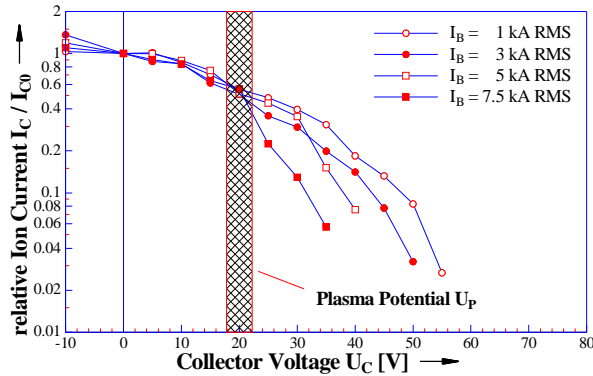


Fig. 6b: I_C-U_C -characteristics for AMF-contacts ($I_B = 1$ to 7.5 kA_{RMS}, $U_C = -10$ to +60 V, $g = 0^\circ$, $s = 50$ mm, $t = 2.5$ ms before current zero)

The characteristics for contacts of the RMF-type shows the typical shape with a strong dependence of the individual characteristics on the RMS and momentary currents,

respectively. The change-over between the two sections of the typical RFA-characteristic, the transition- and retarding area, is evident by a point of inflection. This point of inflection slides to higher collector voltages (e.g. higher ion energies) with increasing arc current I_B . According to equ. 7 the ion energy distribution can be described by the slope of the characteristic in the retarding area, which also decreases with the decreasing arc current. The summary of these facts leads to an increase of the ion energy and to shifting of the complete ion energy distribution towards higher voltages with decreasing arc current. This is confirmed by the detection of ions with a maximum energy (I_{Cmax}) equivalent to collector voltages up to +70 V at an arc current $I_B = 1$ kA_{RMS}, in comparison with the maximum voltage for ion detection of +40 V for a arc current $I_B = 8.75$ kA_{RMS}, representing the difference between the ion energy according to the arc current. Deviating from these typical characteristics for RMF-contacts the current dependence of the characteristics for AMF-contacts is less pronounced (figs. 5 and 6b). The typical point of inflection is not pronounced, in comparison to the typical RMF-characteristics. The steepest slope of the characteristics, indicating the maximum of energy distribution, is always positioned close to the plasma potential. The voltage for the detection of I_{Cmax} is +55 V for an arc current of 1 kA_{RMS}, reducing to a voltage of +35 V for the detection of I_{Cmax} for $I_B = 7.5$ kA_{RMS}. Fig. 7a and 7b compares the evaluated ion energy distributions (related to the plasma potential) for the RMF and AMF arrangements. To get the ion energy in eV it was assumed that the ions have a mean charge state $Z=1.8$ [13].

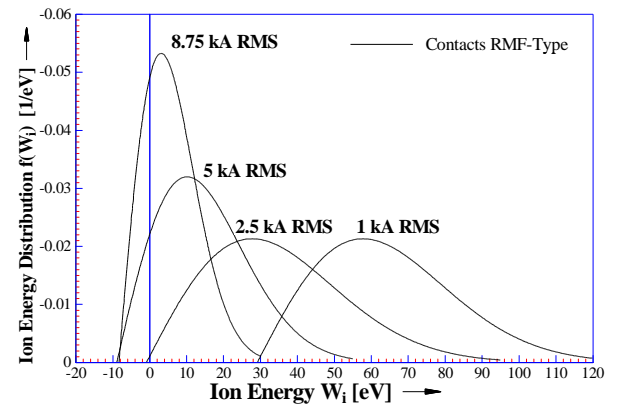


Fig. 7a: Ion energy distribution for RMF-contacts ($I_B = 1$ to 8.75 kA_{RMS}, $U_C = -5$ to +70 V, $g = 0^\circ$, $s = 50$ mm, $t = 2.5$ ms before current zero)

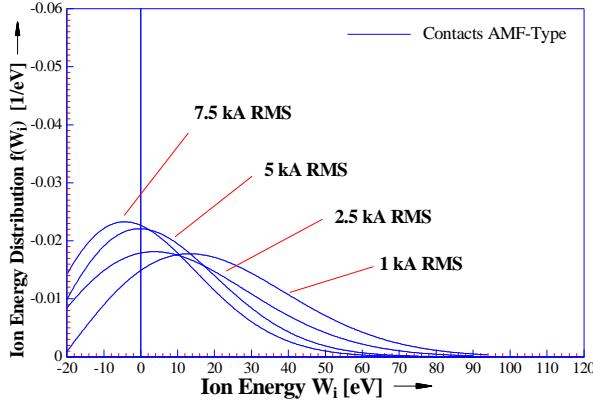


Fig. 7b: Ion energy distribution for AMF-contacts ($I_B = 1$ to $7.5 \text{ kA}_{\text{RMS}}$, $U_C = -10$ to $+60 \text{ V}$, $g = 0^\circ$, $s = 50 \text{ mm}$, $t = 2.5$ ms before current zero)

Generally speaking, these graphs reflect the distribution of the ion speed components directed towards the analyzer. Ideally only positive energy values should exist. However, in the saturation and transition part of the I_C - U_C -curves ions with potentials lower than the plasma potential are superimposed by accelerated ions. This acceleration depends on the potential gradient between the two separation grids and the collector voltage below the plasma potential. The branch of the energy distribution for ions with an energy value below zero consists of these accelerated ions, ions diffusing in the RFA through the aperture and ions, dispersed by the separation grids flying towards the collector.

The peak of the energy distribution, related to the plasma potential, lies close to zero for currents above $5 \text{ kA}_{\text{RMS}}$ for both contact types. This distribution is close to a Maxwellian energy and velocity distribution, respectively, with its peak at zero speed, meaning that the direction of ion motion is at random. This is characteristic for a plasma where collisions determine the particle behavior [7]. On RMF contacts there is a very pronounced shift towards high energy peaks for lower currents, meaning that under these conditions the ions are strongly directed from the arc between the contacts towards the analyzer. As shown by analyzer measurements with different detection angles g [7] they originate from the cathode spots and move outwards more or less freely. The velocity of these ions can be evaluated up to 10^4 m/s [7]. For lower arc currents and a decreasing plasma density the probability of collisions in the inter-electrode space decreases.

With AMF contacts the distribution maximum shifts only moderately to the right for low arc currents, quite in contrast to RMF contacts. While on the RMF arrangement the width of the distribution is narrower for higher arc current, the width remains nearly unchanged for AMF contacts. Using these contacts, the arc stays in a diffuse mode up to higher arc currents. In comparison to contacts of the RMF-type, the axial magnetic field forces the charge carriers in a gyration round the magnetic flux lines. Thus the probability of collisions in the inter-electrode space increases, and the character of the distribution is much more Maxwellian even for small currents. For higher arc currents, the increasing plasma density further enhances the probability of collisions in the contact gap.

3.3 Ion energy distribution of AMF arcs in varying distance from the electrodes

In experiments with RMF-contacts the variation of the analyzer distance s from the contacts shows a decreasing ion density n_i , in first approximation by $1/s^2$. Using AMF-contacts, this decreasing density according to the increasing distance is superimposed by an additional effect which is assumed to be caused by the axial magnetic field which is directed oppositely in the areas between the contacts and in some distance outside them. In between there is a magnetically neutral zone. Fig. 8 shows ion energy distributions for two distances and different times before current zero (i.e. different momentary arc currents).

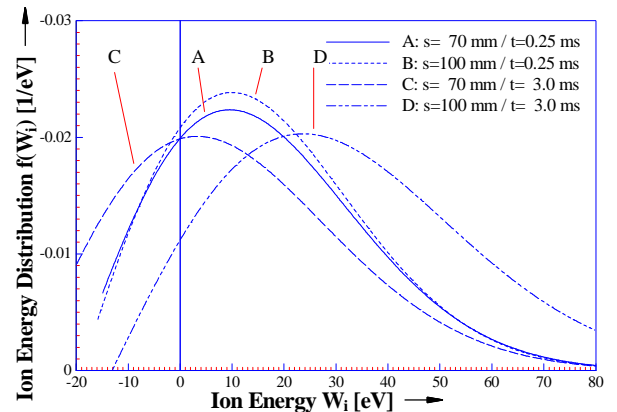


Fig. 8: Ion energy distribution of AMF-contacts with varying distances s ($I_B = 3 \text{ kA}_{\text{RMS}}$, $U_C = -10$ to $+60 \text{ V}$, $g = 0^\circ$, $s = 70 / 100 \text{ mm}$, $t = 0.25 / 3 \text{ ms}$ before current zero)

For a distance of $s = 70$ mm, due to the described results in Chapter 3.1 with $s = 50$ mm, the ion energy distribution shifts towards lower energy values with an increasing arc current (A to C), representing a "thermal" energy distribution (C). The measured distribution with the RFA positioned with a distance $s = 100$ mm is similar for lower arc currents (0.25 ms before current zero), but with an increasing arc current this function shifts towards higher energy values.

The measured ion energies can also be expressed in terms of ion velocities according to $W_i = \frac{1}{2} m_i v_i^2$. In fig. 9 this speed is plotted vs. the momentary arc current $i_B(t)$ for experiments similar to those of fig. 8.

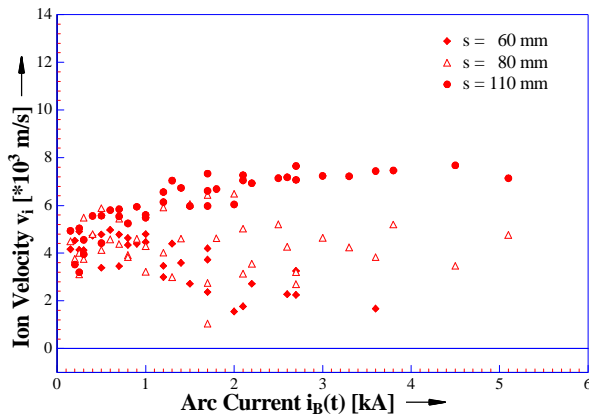


Fig. 9: Ion velocity v_i of AMF-contacts with different distances s between contacts and analyzer ($i_B(t) = 0.1$ to 5.2 kA, $U_C = -10$ to $+60$ V, $g = 0^\circ$, $s = 60 / 80 / 110$ mm)

For lower values of the arc current the ion velocity is nearly independent of the arc current. With increasing arc current and a large distance s , opposite to lower distances, the ion velocity increases and reaches values up to $8 \cdot 10^3$ m/s. Due to the position of the RFA with its visual line directed towards the contact axis, only ions with a velocity component in this direction can be detected. Ions leaving the contact gap with tangential velocity. It is assumed that because of the inhomogeneous field outside the contact gap (the direction becomes zero and reverses), this gyration changes to a linear, approximately collision-free motion in a certain radial distance. The radial ion speeds reach values that are comparable with the maximum ion velocities detected for RMF-contacts.

4. Summary and conclusions

The energy distribution of ions in the vacuum arc plasma during the last 3 ms before current zero has been investigated by means of a retarding field analyzer. Significant differences could be observed between RMF and AMF contacts. For currents above 5 kA the distribution in both cases resembles a Maxwellian distribution, characteristic for a plasma whose particle motion is determined by collisions. For arcs between RMF contacts the ion motion is shifted towards a collisionless motion directed radially outwards with decreasing current. On contrast, the energy distribution of AMF plasma ions stays much closer to the collision-dominated Maxwellian pattern for low currents. This is attributed to the increasing collision frequency caused by the charge carrier gyration and plasma confinement due to the axial magnetic field. An interesting observation about the influence of the analyzer position on the measured energy distribution of AMF arcs is also explained by the ion motion in the magnetic field configuration.

Acknowledgements

The authors gratefully acknowledge the support by the Deutsche Forschungsgemeinschaft DFG.

References

- [1] Biewendt, V., "Einfluß der Schirm- und Kontaktgeometrie auf das Löschvermögen von Vakuumleistungsschaltern", Thesis, Techn. Univ. Braunschweig, Germany, 1993
- [2] Fenski, B., "Verhalten von Axialmagnetfeldkontakten in Vakuumleistungsschaltern", Thesis, Techn. Univ. Braunschweig, Germany, 1997
- [3] Lafferty J.M. (Editor), "Vacuum arcs - theory and application", John Wiley & Sons, New York 1980
- [4] Anders A., Anders S., Jüttner B., Böttcher W., Lück H., Schröder G., "Investigation of cathode spots by Laser absorption Photography", Proc. 15th ISDEIV, Darmstadt, Germany, 1992, p. 653
- [5] Hantzsche E., "A simple model of diffuse arc plasma", Contrib. Plasma Phys. 30, 1990, p. 575

- [6] Kimblin C.W., "Erosion and ionisation in the cathode spot regions of vacuum arcs", J. Appl. Phys., Vol. 44, No. 7, 1973, p. 3074
- [7] Rusteberg C., "Bestimmung von Plasmaparametern in Vakuum-Hochstrombögen", Thesis, Techn. Univ. Braunschweig, Germany, 1993
- [8] Lindmayer M., Rusteberg C., Jüttner, B., Pursch, H.: "On the ion energy distribution of high current arcs in vacuum", IEEE Trans. on Plasma Science Vol. 25 (1995) pp. 909-914.
- [9] Lindmayer M., Rusteberg C., Klajn A.: "Measurement of the plasma parameters of high current arcs in vacuum", Proc. 7th Int. Conf. Switching Arc Phenomena, Lodz, Poland, 1993, p. 326
- [10] Propopenko S.M.L., Laframboise J.G., Goodings J.M., "Evaluation of an orifice probe for plasma diagnostics", J. Appl. Phys., Vol. 5, p. 2152
- [11] Ivanov V.A., Konyshov M., Anders S., Jüttner B., Pursch H., Sünder D., "On the energy of electrons and ions of a pulsed metal vapour arc in vacuum", Akad. d. Wiss. der DDR, Zentralinstitut für Elektronenphysik, 1990
- [12] Pitts R.A., "Ion energy, sheath potential and secondary electron emission in the Tokamak Edge", Thesis, Univ. of London, Great Britain, 1990
- [13] Brown I.G., Godechot X., "Vacuum arcs ion charge state distributions", IEEE Trans. Plasma Science, Vol. PS-19, Nr. 5, 1991

The authors are indebted to Deutsche Forschungsgemeinschaft (German Research Foundation) for supporting this work.